



# The Hyrax appliance with tooth anchorage variations in surgically assisted rapid maxillary expansion: a finite element analysis

Flavio Henrique Silveira Tomazi<sup>1</sup> · Ricardo Augusto Conci<sup>2</sup> · Claiton Heitz<sup>1</sup> · Pedro Yoshito Noritomi<sup>3</sup> · Luciane Macedo de Menezes<sup>1</sup> · Eduardo Martinelli Santayana de Lima<sup>1</sup> · Eduardo Rolim Teixeira<sup>1</sup>

Received: 17 January 2022 / Accepted: 10 August 2022

© The Author(s), under exclusive licence to Springer-Verlag GmbH Germany, part of Springer Nature 2022

## Abstract

**Purpose** It is known that a correct transverse maxillary dimension is a key factor for a stable occlusion, which brings functional and esthetic benefits for the patient. In patients presenting maxillary atresia and the completion of bone growth, a highly recommended option for correction is the surgically assisted rapid maxillary expansion (SARME) associated with the Hyrax appliance. The objective of this study was to evaluate the influence of tooth anchorage variations of the Hyrax appliance in SARME through finite element analysis, evaluating which anchorage option might be associated with more effective orthopedic results with less undesired side effects.

**Methods** Five different dental anchoring conditions for the Hyrax appliance were simulated through FE analysis applying premolars and molars as anchorage, having the same force applied by the activation of the Hyrax screw (0.5 mm) in all groups. The maxillary displacement results (axes X, Y, and Z) and generated stresses for both teeth and maxillary bone were calculated and represented using a color scale.

**Results** All groups presented significant bone displacement and stress concentration on anchoring teeth, with the group presenting anchorage in the 1st and 2nd molars showing the greatest maxillary horizontal displacement (axis X) and suggesting the lowest tendency of dental vestibular inclination.

**Conclusions** Variations in dental anchorage might substantially affect the maxillary bone and teeth displacement outcome. The protocol for the Hyrax apparatus in SARME applying the 1st and 2nd molars as anchorage might generate less tilting and inclination of the anchoring teeth.

**Keywords** Hyrax · Tooth anchorage · Maxillary expansion · Finite element · Bone displacement

## Introduction

Adequate transverse maxillary dimension is a critical component of a stable and functional occlusion [1]. Posterior crossbite has an incidence of 9.4% in the population, but it rises up to 30% in the group of patients who need orthognathic surgery [2]. Typically, adults with a transverse

deficiency of the maxilla show both a deep palate and a narrow upper dental arch [3]. A predictable treatment approach for this condition would be the surgically assisted rapid maxillary expansion (SARME), described as an effective procedure with predictable results [4].

SARME is usually applied using tooth-borne, tooth-tissue-borne, or bone-borne devices. The Hyrax expander (tooth-borne) has been pointed as the most common appliance used for SARME [4, 5]. However, some undesired side effects of SARME performed with the Hyrax screw were described, including gingival dehiscence, fenestration, bone loss, and/or root resorption [6]. These side effects might show a wide range of variations, associated mainly to distinct surgical approaches, design of expanders, and patient features [7, 8].

The application of finite element (FE) analysis on studies of vectorial forces in orthodontics has been associated

✉ Eduardo Rolim Teixeira  
eduardo.teixeira@puers.br

<sup>1</sup> School of Health and Life Sciences, Pontifical Catholic University of Rio Grande Doo Sul, Av. Ipiranga 6681, Predio 06 Bairro: Partenon, Porto Alegre, RS 90619-900, Brazil

<sup>2</sup> Department of Oral Surgery, State University of Western Parana, Cascavel, Parana, Brazil

<sup>3</sup> 3D Technologies Division, Renato Archer Technology Information Center, Campinas, São Paulo, Brazil

with several advantages. Namely, it is a noninvasive technique; the actual amount of stress experienced at any given point might be theoretically measured; structures like teeth, alveolar bone, periodontal ligament, TMJ, and craniofacial bones, among others, may be mathematically simulated, having their mechanical properties virtually assigned; eventual displacement of teeth can be visualized graphically; physiological forces may easily be simulated as to their point of application, magnitude, and direction; and last, it allows the possible repetition and/or modification of the investigation as necessary [9]. Following these assumptions, FE models have also been applied to investigate through mathematical simulations the possible effects of SARME with different surgical and anchorage approaches on the dental and skeletal structures [7].

It is known that specific designs of appliances used in SARME may generate forces usually transmitted to the neighboring tissues. Bone-borne devices are expected to transmit forces and generate displacements to the adjacent bones and their sutures [10, 11]. These generated forces might also induce undesired teeth movements as well, causing side effects that might negatively influence treatment outcomes.

Previous studies that investigated SARME using FE models have focused mainly on the stresses associated with distraction movements in craniofacial bones, namely sphenoid, frontal, temporal, nasal, and occipital bones and their respective sutures [12]. To our knowledge, no studies have applied FE models to evaluate the effects of SARME on the maxillary bone and teeth using different types of tooth anchorage. Therefore, this investigation was designed to analyze through FE models the possible effects of different types of tooth anchorage in SARME applying the Hyrax screw. The null hypothesis assumed here was that the created FE models with distinct types of tooth anchorage used for SARME will generate no differences on loading characteristics between them.

## Methods

The present investigation protocol was approved by the Research Committee of the School of Health and Life Sciences of the Pontifical Catholic University of Rio Grande do Sul (PUCRS – No. 8241).

The FE method was applied to build mathematical models to simulate the effects of SARME on supporting bone and teeth using the hyrax expander, applying 5 distinct types of tooth-borne anchorage, each representing a distinct test group. Overall, each generated 3D tetrahedral-based element FE model simulated geometrically the maxillary bone, soft tissue, and anchoring teeth, as well as the Hyrax screw and their respective mechanical properties (Figs. 1 and 2). Total

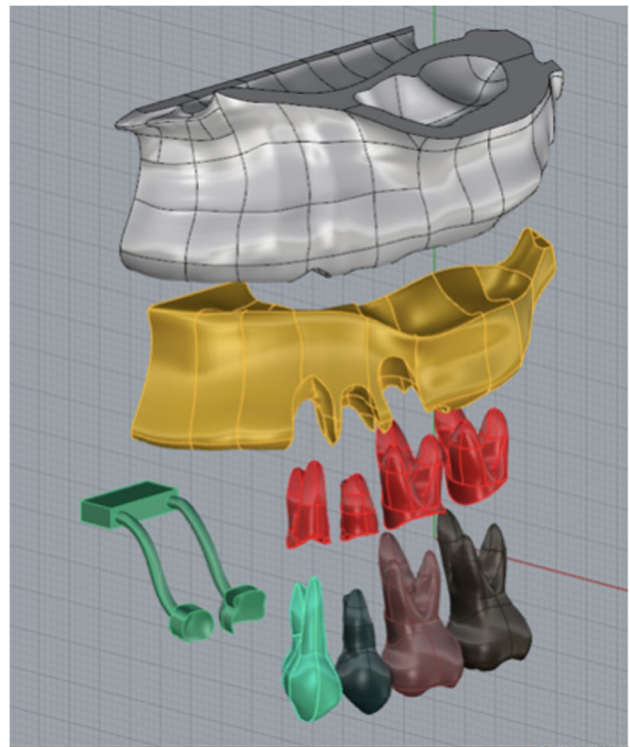


**Fig. 1** Schematics of the main structures represented in the FE models, being cortical bone, cancellous bone, periodontal ligament, teeth, and the Hyrax appliance, in order of appearance from figure top to bottom

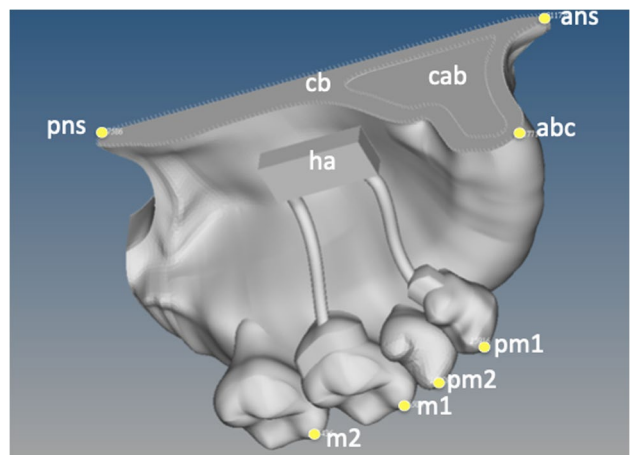


**Fig. 2** Represented structures and selected points (yellow dots) to calculate node displacement on each modeled structure, representing the Hyrax appliance (ha) the second molar mesial buccal cusp tip (m2), first molar mesial buccal cusp tip (m1), second premolar buccal cusp tip (pm2), first premolar buccal cusp tip (pm1), cortical bone (cb), alveolar bone crest (abc), cancellous bone (cab) anterior nasal spine (ans), and posterior nasal spine (pns)

number of elements and nodes of each created model and for each individual model component are shown in Table 1.

**Table 1** Total number of elements and nodes of the created models for each analyzed group and their designed constituents

	Number of elements	Number of nodes	Tooth anchorage
Cortical bone	335,781	1,343,124	
Cancellous bone	110,870	443,480	
Periodontal ligament	426,358	1,705,432	
1 <sup>st</sup> Premolar	70,927	283,708	
2 <sup>nd</sup> Premolar	92,351	369,404	
1 <sup>st</sup> Molar	141,162	564,648	
2 <sup>nd</sup> Molar	284,838	1,139,352	
Group 1	98,979	395,916	1 pm + 1 m
Group 2	82,457	329,828	1 pm + 2 m
Group 3	77,355	309,420	2 pm + 2 m
Group 4	108,125	432,500	1 m + 2 m
Group 5	99,234	396,936	2 pm + 1 m
TOTAL	1,928,437	7,713,748	

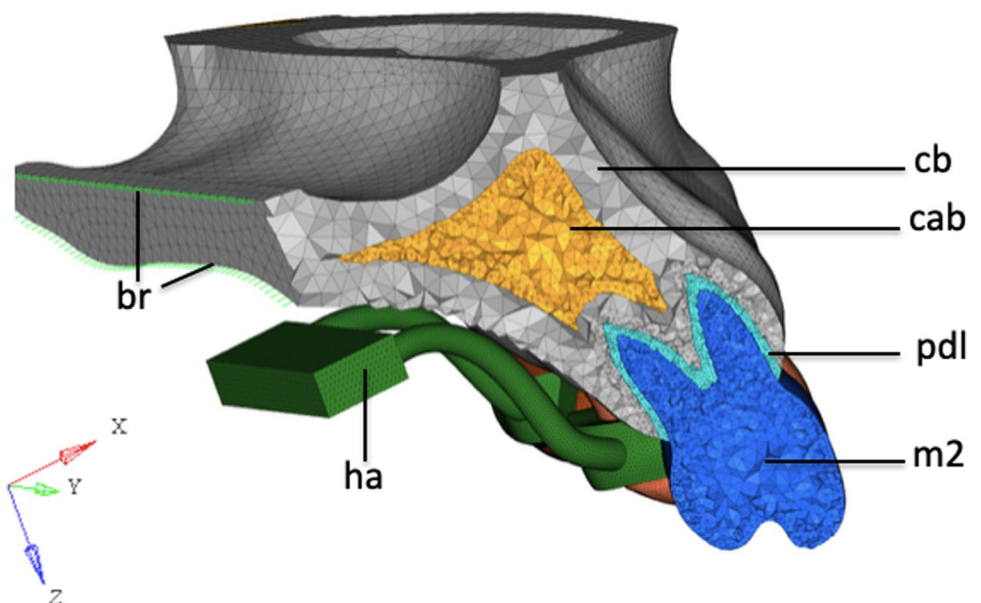
**Table 2** Assumed Young’s modulus and Poisson’s ratio values of the represented FE structures

	Young’s modulus (MPa)	Poisson’s ratio
Cortical bone	$1.4 \times 10^4$	0.3
Cancellous bone	$1.4 \times 10^3$	0.3
Teeth	$2.6 \times 10^4$	0.3
Periodontal ligament	50	0.49
Stainless steel (Hyrax)	$2.1 \times 10^5$	0.35
Oral mucosa	$6.8 \times 10^{-1}$	0.45

The represented 3D geometry of the maxilla was obtained from the CT DICOM data of a dry human skull, obtained with a CT slice thickness of 1 mm (Information Technology

Center—CTI—CenPRA, Campinas—SP, Brazil), along with the Hyrax screw created based on its designed dimensions (11.5 mm in length, 5 mm in width, 2 mm in height) and mechanical properties (Table 2) as informed by the manufacturer (Dental Morelli, SP, Brazil). FE model meshing was generated using a specific computer meshing software (Rhinoceros 5.0, McNeel, Seattle, WA, USA) (Fig. 3). Then, FE models were created and analyzed by applying specific boundary restrictions (Fig. 3) and loading simulations generated by a total activation of 1 mm of the Hyrax screw, having their calculations run using a specific software (Altair HyperWorks 2017, Altair engineering, Michigan – MI, USA). The mechanical properties of all simulated tissues and Hyrax screw were considered as being homogeneous, isotropic, and linear elastic. Young’s modulus and Poisson’s ratio values for bone, teeth, soft tissue, and Hyrax

**Fig. 3** Finite element model meshing of the maxilla, indicating the representation of the Hyrax appliance (ha), the second molar (m2), cortical bone (cb), periodontal ligament (pdl), cancellous bone (cab), and the boundary restrictions (br) and bar elements (green dotted line). Red, yellow and blue arrows indicate the X, Y, and Z axes of displacement, respectively



screw were assumed as suggested [7, 8] or as indicated by the manufacturer (Table 2).

Five FE models simulated different types of tooth anchorage and formed the tested groups, being G1, anchored at first premolar and first molar ( $4_s-6_s$ ); G2, at first premolar and second molar ( $4_s-7_s$ ); G3, at second premolar and second molar ( $5_s-7_s$ ); G4, at first molar and second molar ( $6_s-7_s$ ); and G5, at second premolar and first molar ( $5_s-6_s$ ) (Fig. 4).

The analysis of SARME effects was simulated based on displacement from the center of the Hyrax screw after an assumed screw activation of 1 mm (4/4-screw turns), based on a regular one-day screw activation protocol, generating a resultant 0.5 mm lateral movement for each side of the maxilla. All tested groups simulated a Le Fort I osteotomy, with midline (sagittal) split, no fracture of the pterygoid plate and no bone contact along the osteotomy. Preservation of the union between the maxilla to the pterygoid plate represented here a more simplified surgical technique applied regularly in SARME. Bone segments of the maxilla could move freely, without friction, in the transverse (X), sagittal (Y), and vertical (Z) axis. FE model restraints were established to simulate a symmetry in the maxilla's midline, along with total displacement restriction in the mid portion of the pterygoid bone (Fig. 3). Also, a possible resistance to the maxillary opening movement offered by the palatal mucosa was simulated applying bar elements with their unidirectional movement characteristics (X axis) to the midline suture, to simulate any possible displacement opposing features and allowing proper adjustments of their mechanical properties and node restraints for each tested group (Fig. 3).

The SARME effects on bone and teeth were translated as displacements of specific anatomic points in the X, Y, and Z axes (07 selected nodes), being abc, alveolar bone crest (node 211,771); ans, anterior nasal spine (node 211,729); pns, posterior nasal spine (node 217,586); pm1, first premolar buccal cusp tip (node 15,916); pm2, second premolar buccal cusp tip (node 191,096); m1, first molar mesial buccal cusp tip (node 596,505); and m2, second molar mesial buccal cusp

tip (node 196,436) (Fig. 2). Also, representations of the cortical bone (cb), cancellous bone (cab), and the Hyrax appliance (ha) were designed as shown (Fig. 2). A color scale was applied to visually display the displacement results verified at the anatomic points for each simulated group.

## Results

Displacements of the anchoring teeth and the chosen anatomic structures along each displacement axis are shown in Table 3. SARME effects over bone and teeth were mostly through the X axis in all 5 tested groups. Alveolar bone crest (abc) moved 57–63% of the displacement generated in the Hyrax screw (0.5 mm), whereas ans moved 34–37% and pns remained almost unchanged (2%). The most significant tooth displacement in X axis occurred on pm1, reaching 64–74% of the screw dislocation. However, m1 and m2 presented displacement as much as pm1 in G4 ( $6_s-7_s$ ).

In Y axis, displacements in bone were greater in abc (14–16%) compared to ans (9–10%) or pns (10%). All groups showed displacements in pm1, which were greater when pm1 was an anchoring tooth (G1, 10%; G2, 13%). On the other hand, none of the groups showed displacement of m2 in Y axis.

In Z axis, the displacement was greater in pns (16–20%) than ans (0–10%) or abc (5–10%). The m2 displacement was 19–27% of the Hyrax screw-induced force, whereas in pm1 was 10–19%.

All groups showed greater displacement in the anterior region in comparison to the posterior region. There was a tendency of a “V-shaped” opening of the maxilla, with a posterior vertex in the intermaxillary suture. Group 4 ( $6_s-7_s$ ) showed the greatest displacement along the X axis compared to all other groups (Fig. 5).

In the Z axis, all groups showed a downward displacement of the anterior region and upward displacement of the posterior region. The changes were again greater in group 4 ( $6_s-7_s$ ) compared to all other groups (Fig. 6).

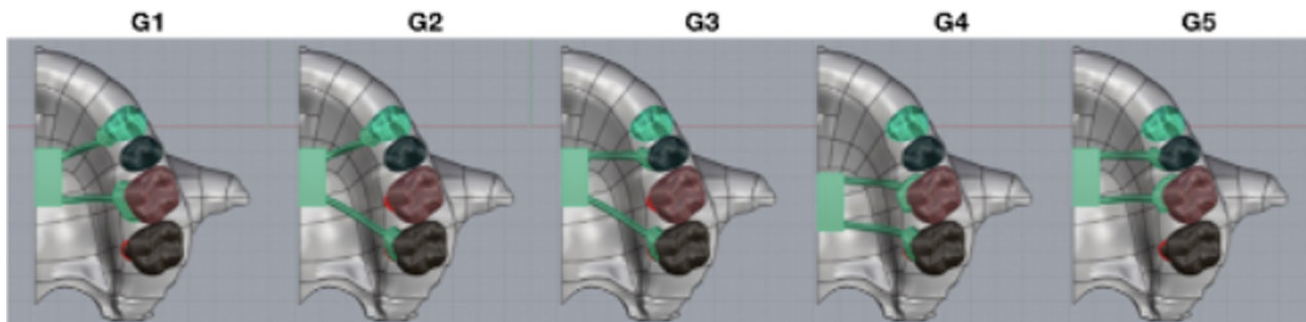
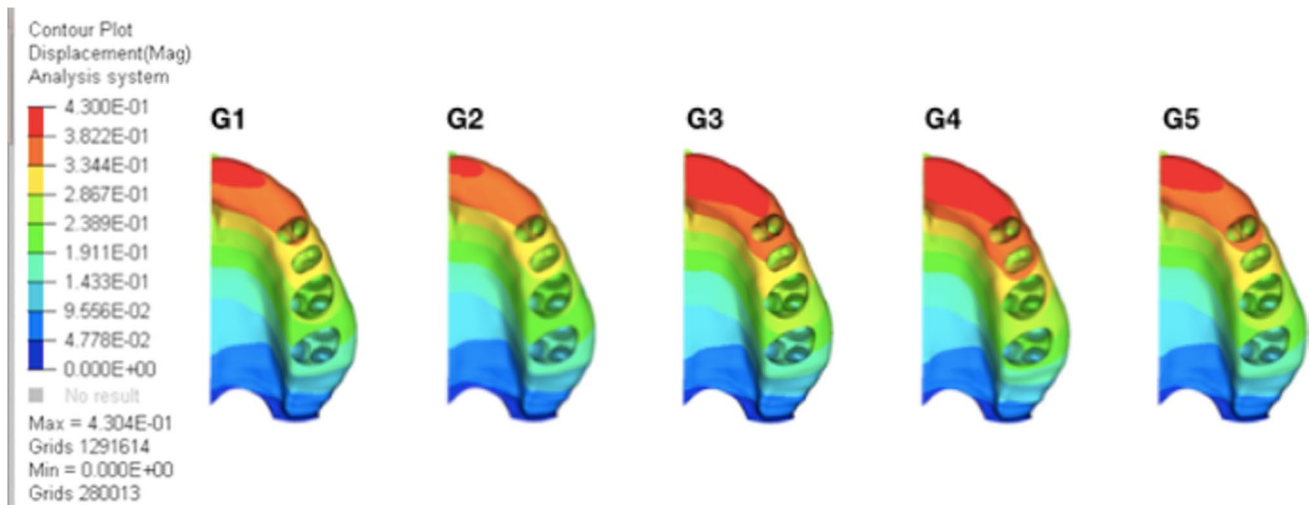


Fig. 4 Variations of the tooth anchorage of the Hyrax appliance represented in each tested group

**Table 3** Quantitative displacement of all represented structures in X, Y, and Z axes in the 5 analyzed groups (mm)

	G1	G2	G3	G4	G5
1 <sup>st</sup> Premolar	X 0.325	X 0.372	X 0.320	X 0.348	X 0.337
	Y 0.050	Y 0.063	Y 0.029	Y 0.025	Y 0.032
	Z -0.059	Z -0.053	Y -0.081	Z -0.082	Z -0.087
2 <sup>nd</sup> Premolar	X 0.286	X 0.277	X 0.253	X 0.325	X 0.276
	Y 0.017	Y 0.017	Y -0.003	Y 0.011	Y 0.045
	Z -0.096	Z -0.093	Z -0.065	Z -0.105	Z -0.071
1 <sup>st</sup> Molar	X 0.320	X 0.245	X 0.262	X 0.338	X 0.321
	Y 0.036	Y 0.001	Y 0.001	Y -0.003	Y 0.034
	Z -0.121	Z -0.105	Z -0.111	Z -0.124	Z -0.130
2 <sup>nd</sup> Molar	X 0.197	X 0.293	X 0.278	X 0.359	X 0.214
	Y 0.002	Y -0.032	Y -0.012	Y -0.008	Y -0.002
	Z -0.094	Z -0.107	Z -0.111	Z -0.136	Z -0.102
Anterior nasal spine	X 0.171	X 0.169	X 0.172	X 0.172	X 0.183
	Y 0.046	Y 0.045	Y 0.046	Y 0.045	Y 0.049
	Z 0.021	Z 0.018	Z 0.026	Z 0.047	Z 0.025
Alveolar bone crest	X 0.291	X 0.284	X 0.296	X 0.316	X 0.313
	Y 0.074	Y 0.074	Y 0.073	Y 0.070	Y 0.079
	Z 0.024	Z 0.020	Z 0.028	Z 0.049	Z 0.027
Posterior nasal spine	X -0.009	X -0.008	X -0.009	X -0.010	X -0.010
	Y 0.051	Y 0.049	Y 0.051	Y 0.051	Y 0.055
	Z 0.078	Z 0.077	Z 0.082	Z 0.097	Z 0.084



**Fig. 5** Displacement of represented structures along the X axis observed in all groups (in mm)

Considering the resultant stresses generated in neighboring teeth and tissues, traction forces in the anchoring teeth generated a trend towards an anticlockwise rotation of the molars, as seen in groups 3 and 4. Among the groups in which the second premolars were used as anchorage (G3 and G5), a tendency towards traction and extrusion on these teeth could be hypothesized, as indicated by the verified von Mises stress concentration color diagram (Fig. 7).

### Discussion

Rapid maxillary expansion (RME) is an established and well-documented treatment option when considering maxillary transverse deficiencies, particularly in patients presenting skeletal maturity [13]. However, the involved loads and recurrent undesired side effects to which teeth and craniofacial bones are frequently subjected have not been clearly

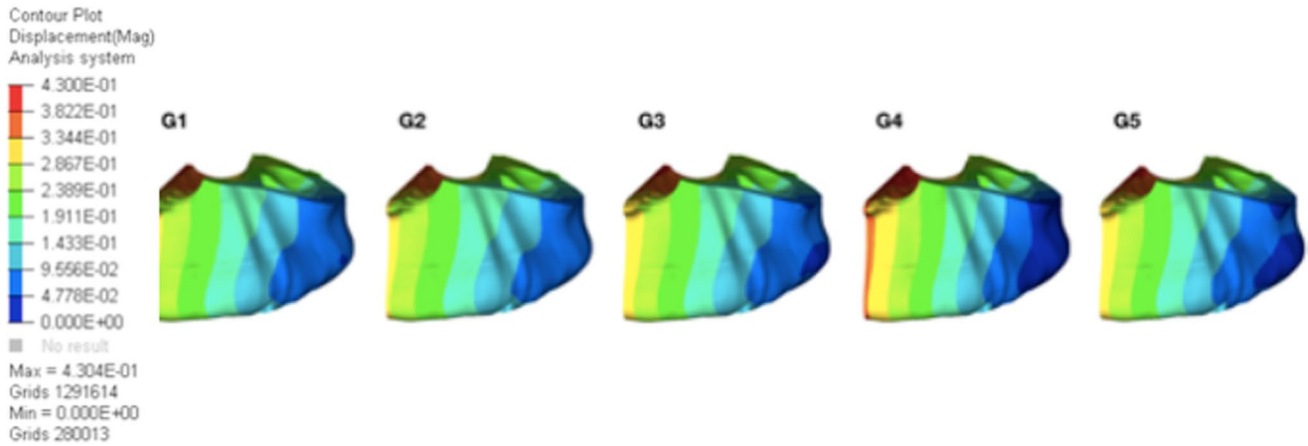


**Fig. 6** Displacement of represented structures along the Z axis for all groups (in mm)

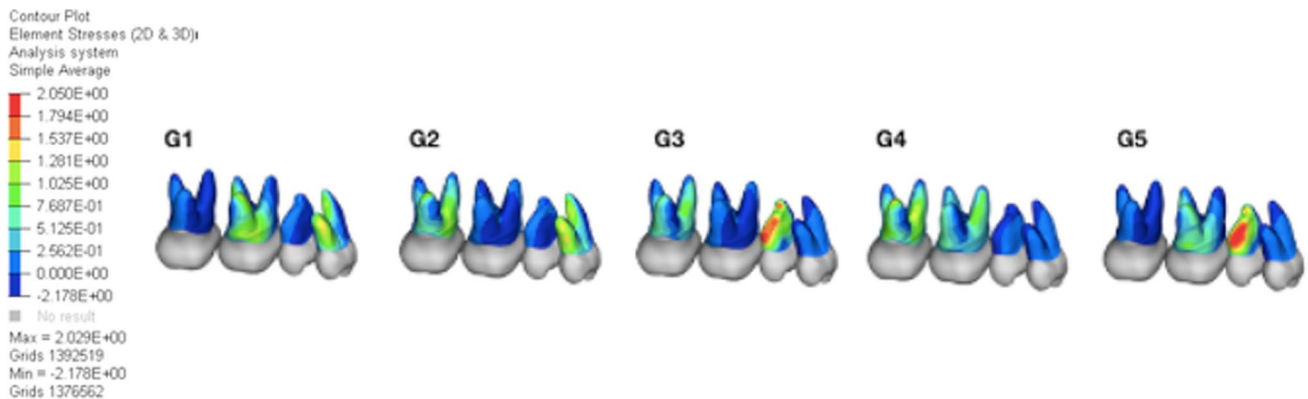


**Fig. 7** Stress distribution (von Mises) in the roots of each anchoring teeth for all the tested groups (MPa)

investigated, mainly due to the limitations of methods to evaluate and quantify these alterations *in vivo*. The applied finite element method might represent a viable alternative to simulate *in vitro* those involved forces and consequent displacements and to speculate on the possible consequences of their application on the involved living structures.

Previous studies applying similar FE analyses investigated the influence of force distribution and structural displacements for maxillary expansion through variations in the expanding screw positioning on the Hyrax apparatus anchored mainly in the maxillary 1<sup>st</sup> premolars and the 1<sup>st</sup> molars, and pointed out that there might be a difference in the distribution of forces influencing the clinical outcome depending on the screw position in relation to the maxillary arch [11]. To our knowledge, the present investigation might represent the first attempt in the literature to compare through FE method the displacement of the living structures in maxillary expansion involving tooth anchorage variations of the Hyrax appliance.

The analysis of the obtained results regarding the transverse displacement of the maxilla in all groups usually

presented a greater anterior and a smaller posterior expansion of the maxilla when considering an occlusal view, corroborating previous studies which observed a marked gain in the active phase of the expansion, with a larger opening of the anterior region followed by a reduced opening in the posterior region [9, 10]. Also, at frontal view (X axis), it also displayed a V-shaped pattern of expansion, with its vertex turned towards the posterior nasal spine. When considering an occlusal view (Z axis), the same V-shaped pattern appears, with its vertex apparently turned towards the glabella, as a probable consequence of the resultant vector of the X and Y axes displacements [9]. In the present investigation, G4 showed the highest values in terms of transverse displacement of the maxilla, possibly due to the applied expansion movement being directed towards the posterior region. This finding was also corroborated by other studies which showed that a more posterior positioning of the expansion device should produce a more parallel opening of the maxilla [14].

Another observation present in all tested groups was the downward displacement of the medial portion of the maxilla

and the upward displacement of its lateral portion. This is in accordance to other reported findings [15–17] which observed that, regarding the palatal plane, a downward displacement along with a downward and backward rotation of the maxilla might occur following its rapid expansion. Considering the present results, all the analyzed groups showed a slightly anterior displacement of the maxilla. Previous studies confirmed also that an anterior displacement of the maxilla might regularly be observed following a palatal disjunction, which may return to its pre-disjunction values at the end of the post-surgical maxillary leveling period [18]. Also, it has been stated that negative values (backward displacement) might also be observed in the supporting teeth probably as a consequence of the applied movement direction.

In the present investigation, we chose to keep a constant vertical position of the expander screw of the Hyrax device. As previously reported, alterations on the screw position might affect teeth and their surrounding tissues, as substantial changes in direction of the resultant forces might be generated [11]. Also, other investigations suggested that the closer the expander device is to the palate, the greater the tendency for teeth extrusion and buccal crown tipping [18].

A consensus may be verified in the literature stating that teeth-supported appliances may promote undesired effects such as vestibular movement of the anchoring teeth and resorption of the buccal bony wall [7, 8, 19]. In the present study, resultant displacements that might indicate a tendency of tooth extrusion might be observed, especially when including the 2<sup>nd</sup> premolar as anchorage as seen in groups G3 and G5, possibly due to its reduced root area. Smaller stress values, a possible indicative of less dental movement, were found in G4 when applying only molars as anchorage, suggesting a positive effect of a larger root area on undesired movements of the anchoring teeth. Also, we consider that the simulation of soft tissues, meaning the applied presence of oral mucosa by the use of bar unidirectional elements at the maxilla midline sagittal split and periodontal ligament element representation could not affect qualitatively the verified stress distribution. Our findings corroborate previous reports on the Hyrax device in SARME, where a greater buccal crown tipping tendency in anchored premolars (8.3°) compared to molars (0.9°) was observed [20, 21].

When premolars were applied as anchorage of the Hyrax expansion device, results of stress concentration suggested a possible tendency of their buccal crown tipping, as resulting forces generated stress concentration also at the buccal bony cortex. On the other hand, when a simulated molar anchorage was applied (G4), it displayed greater tendency of bony displacement with less crown positive inclination, confirmed by von Mises stress concentrations that showed lower stress values at the involved roots. Furthermore, the rapid activation protocol of the Hyrax expander for SARME simulated

here (1 mm/day) was conceived for adult patients presenting full growth and development of their craniofacial bones and sutures, aiming an effective separation of the maxillary bone segments in a considerably shorter period of time and having similar results compared to the slow expansion protocol (1 mm/week) when considering the possible consequences to the Hyrax supporting tissues [22]. However, as clinical predictions could not be based solely on the theoretical findings like these reported here, further studies should be performed to confirm the present assumptions and, if applicable, establish new clinical standards for a proper tooth anchorage protocol applicable for the Hyrax apparatus in SARME that might lead to less undesired clinical complications.

## Conclusion

The results of the FE method simulations for the tested groups in the present study indicated the following:

1. All tested groups presented maxillary bone displacement at the transverse X axis.
2. A tendency of dental extrusion could be considered particularly when premolars were applied as tooth anchorage.
3. The group with tooth anchorage on 1<sup>st</sup> and 2<sup>nd</sup> molars (G4) presented the greatest maxillary transversal displacement and the least tendency of buccal crown tipping.

**Author contribution** “All authors contributed to the study conception and design. Material preparation, data collection, and analysis were performed by all authors. The first draft of the manuscript was written by Flavio H. S. Tomazi and all authors commented on previous versions of the manuscript. All authors read and approved the final manuscript.”

**Funding** The present study was supported by a Doctoral grant from the National Council for Scientific and Technological Development (CNPq), Brazil.

## Declarations

**Ethical approval** The present investigation protocol was approved by the Research Committee of the School of Health and Life Sciences of the Pontifical Catholic University of Rio Grande do Sul (PUCRS – No. 8241).

**Consent to participate** Due to the in vitro nature of the analyses performed and obtained data in the present study, human consent to participate does not apply.

**Consent to publish** Due to the in vitro nature of the analyses performed and obtained data in the present study, consent to publish does not apply.

**Competing interests** The authors declare no competing interests.

## References

1. Gogna N, Johal AS, Sharma PK (2020) The stability of surgically assisted rapid maxillary expansion (SARME): a systematic review. *J Craniomaxillofac Surg* 48:845–852
2. Zawislak E, Gerber H, Nowak R, Kubiak M (2020) Dental and skeletal changes after transpalatal distraction. *Biomed Res Int*. <https://doi.org/10.1155/2020/5814103>
3. Betts NJ, Vanarsdall RL, Barber HD et al (1995) Diagnosis and treatment of transverse maxillary deficiency. *Int J Adult Orthodon Orthognath Surg* 10:75–96
4. Carvalho PHA, Moura LB, Trento GS, Holzinger D, Gabrielli MAC, Gabrielli MFR, Pereira Filho VA (2020) Surgically assisted rapid maxillary expansion: a systematic review of complications. *Int J Oral Maxillofac Surg* 49:325–332
5. Pereira MD, Prado GP, Abramoff MMF, Aloise AC, Ferreira LM (2010) Classification of midpalatal suture opening after surgically assisted rapid maxillary expansion using computed tomography. *Oral Surg Oral Med Oral Pathol Oral Radiol Endod* 110:41–45
6. Chhatwani S, et al. (2021) Evaluation of symmetry behavior of surgically assisted rapid maxillary expansion with simulation-driven targeted bone weakening. *Clin Oral Investig* <https://doi.org/10.1007/s00784-021-03958-w>
7. Lee KH et al (2014) Stress distribution and displacement by different bone-borne palatal expanders with micro-implants: a three-dimensional finite-element analysis. *Eur J Orthod* 36:531–554
8. Park JU et al (2009) Three-dimensional finite element analysis of stress distribution and displacement of the maxilla following surgically assisted rapid maxillary expansion. *J Cran Maxillofac Surg* 37:145–154
9. Singaraju GB et al (2015) A comparative study of three types of rapid maxillary expansion devices in surgically assisted maxillary expansion. *J Int Oral Health* 7:40–46
10. Möhlhenrich SC et al (2017) Simulation of three surgical techniques combined with two different boneborne forces for surgically assisted rapid palatal expansion of the maxillofacial complex: a finite element analysis. *Int J Oral Maxillofac Surg* 46:1306–1314
11. Fernandes et al (2019) Influence of the hyrax expander screw position on stress distribution in the maxilla: a study with finite elements. *Am J Orthod Dentofacial Orthop* 155:80–87
12. MacGinnis et al (2014) The effects of micro-implant assisted rapid palatal expansion (MARPE) on the nasomaxillary complex—a finite element method (FEM) analysis. *Prog Orthod* 15:52–67
13. Tomazi F et al (2017) Stress distribution and displacement analysis during a surgically assisted rapid maxillary expansion using a bone-borne device a finite element study. *Int J Health Sci* 4:65–66
14. Veerstraten J, Kuijpers AM, Mommaerts MY et al (2010) A systematic review of the effects of bone-borne surgical assisted rapid maxillary expansion. *J Cranio Maxillofac Surg* 38:166–174
15. Boas MC, Silva Filho OG, Capelozza Filho L (1991) Rapid maxillary expansion in the primary and mixed dentitions: a cephalometric evaluation. *Am J Orthod Dentofacial Orthop* 100:171–179
16. Wertz RA (1970) Skeletal and dental changes accompanying rapid midpalatal suture opening. *Am J Orthod* 58:41–66
17. Haas AJ (1961) Rapid expansion of the maxillary dental arch and nasal cavity by opening the midpalatal suture. *Angle Orthod* 31:73–90
18. Araugio RMS et al (2013) Influence of the expansion screw height on the dental effects of the hyrax expander: a study with finite elements. *Am J Orthod Dentofacial Orthop* 143:221–227
19. Jeon PD, Turley PK, Moon HB, Ting K (1999) Analysis of stress in the periodontium of the maxillary first molar with a three-dimensional finite element model. *Am J Orthod Dentofacial Orthop* 115:267–274
20. Baccetti T, Franchi L, Cameron CG, Jr MJA (2001) Treatment timing for rapid maxillary expansion. *Angle Orthod* 71:343–350
21. Pinto et al (2001) Immediate post-expansion changes following the use of the transpalatal distractor. *J Oral Maxillofac Surg* 59:994–1000
22. Proffit, WR, Fields, HW, Sarver, DM, Ackerman, JL. (2013). *Comprehensive orthodontic treatment in the early permanent dentition*. In: *Contemporary orthodontics*. 5th ed. St. Louis (Mo): Elsevier/Mosby.

**Publisher's note** Springer Nature remains neutral with regard to jurisdictional claims in published maps and institutional affiliations.

Springer Nature or its licensor holds exclusive rights to this article under a publishing agreement with the author(s) or other rightsholder(s); author self-archiving of the accepted manuscript version of this article is solely governed by the terms of such publishing agreement and applicable law.